ELSEVIER

Comput. Methods Appl. Mech. Engrg. 191 (2002) 3331–3345

Computer methods in applied mechanics and engineering

www.elsevier.com/locate/cma

Adaptive boundary element method of time-harmonic exterior acoustics in two dimensions

J.T. Chen *, K.H. Chen, C.T. Chen

Department of Harbor and River Engineering, National Taiwan Ocean University, P.O. Box 7-59, 202 Keelung, Taiwan

Received 9 October 2000; received in revised form 31 December 2001

Abstract

In this paper we carry out boundary element computations of the Helmholtz equation in two dimensions, in the context of time-harmonic exterior acoustics. The purpose is to demonstrate cost savings engendered through adaptivity for propagating solutions at moderate wave numbers. The computation are performed on meshes of constant boundary elements, and are adapted to the solution by locally changing element sizes (h-version). Burton and Miller approach is employed to solve the exterior problems for all wave numbers. Two error indicators obtained from the dual integral equations in *conjunction* with the exact error indicator are used for local error estimation, which are essential ingredients for all adaptive mesh schemes in BEM. Computational experiments are performed for the two-dimensional exterior acoustics. The three error tracking curves are in good agreement with their shapes. Three examples show that the adaptive mesh based on the error indicators converge to the exact solution more efficiently using the same number of elements than does uniform mesh discretization.

Keywords: Adaptive boundary element; Exterior acoustics; Hypersingular equation; Error indicators

1. Introduction

Numerical methods are always utilized to solve problems especially when an exact solution is not available. The discretization process, which transforms a continuous system into a discrete system using finite number of degrees of freedom, results in errors. The discretization error is defined as a measure of difference between the exact solution and the numerical approximation. Obtaining a reliable error estimation [3,16–18,22,24] is to guarantee a certain level of accuracy for the numerical results, and is a key factor of the adaptive mesh procedure [3,16,17]. Thus, estimation of the discretization error in the numerical method is the first step in adaptive mesh generation.

The h-version [3,17], p-version [15,17] and r-version schemes [17] have been recently used to improve the accuracy of numerical methods. In the h-version scheme, the total number of elements increases, but the order of the interpolation function remains unchanged. Since the global matrix must be reformulated after

* Corresponding author. Tel.: +886-2-24622192x6140; fax: +886-2-246632375.
E-mail address: jtchen@mail.ntou.edu.tw (J.T. Chen).

0045-7825/02/$ - see front matter
PII: S0045-7825(02)00214-1

mesh refinement, the computational cost becomes very high. In this way, the efficient remesh tactics are required when h-version scheme is adopted. The adaptive tactics for h-version are generally referred to as the reference value method [17], in which the element mesh is refined where the error is larger than the prescribed reference value. This provides a criterion to determine where the elements should be divided into more partitions by finding the residuals in the integral equation pointwisely.

A large number of studies on adaptive BEM have been done by Kamiya et al. [16], using sample point error estimation. However, the error stems not only from the discretization procedure, but also from the mismatch of the collocation points on the boundary. Zarikian et al. [24] and Paulino et al. [21,22] used pointwise error estimation to study the *convergence* of the interior problem by using the hypersingular residuals. Both the singular integral equation (UT) and *hypersingular* integral equation (LM) in the dual BEM can independently determine the unknown boundary data for the problems without a degenerate boundary [4]. The residuals obtained from these two equations can be used as indexes of error estimation. This provides a guide for remeshing without the problem of mismatch of the collocation points on the boundary in the sample point error method. By creating more divisions in the boundary mesh where the estimated error is large, the error curve will change where the error is redistributed. Therefore, Liang et al. [19] applied the hypersingular equation to find the residual for error estimation in the Laplace equation. Both interior and exterior problems were considered.

In studying the exterior acoustics as shown in Fig. 1(a), finite element method in conjunction with the Dirichlet to Neumann (DtN) technique was found to be competitive [13,14] in comparison with BEM. Later, adaptive FEM was extended to solve the problems more efficiently [12,13,23]. For the practical engineers, BEM is more attractive since the model creation takes fewer time for one-dimension reduction. The mesh of DtN FEM and the BEM mesh are shown in Fig. 1(b) and (c), respectively. Although BEM results in fictitious frequency [9], it can be overcome by employing the Burton and Miller formulation. Here, we will focus on the adaptive BEM for exterior acoustics in two dimensions.

In this paper, the Burton and Miller formulation by combining the dual boundary integral equations is utilized to solve the exterior acoustics problems for all wave numbers in order to avoid the problem of

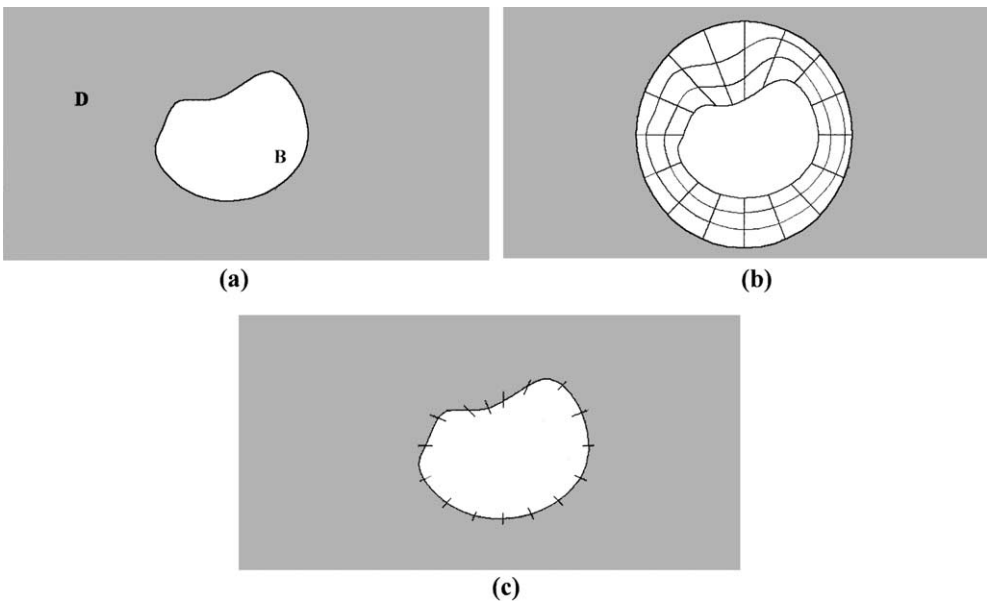

Fig. 1. (a) An unbounded domain with a smooth internal boundary, (b) DtN FEM mesh, (c) BEM mesh.

fictitious frequency. Two residuals, derived by the nonzero terms, which are calculated by substituting the boundary data obtained previously from the Burton and Miller method and known boundary data into the singular and hypersingular integral equations, are found. According to the residuals by collocating the points along the boundary, error tracking curves can be constructed. Based on the error indicators, adaptive scheme can be considered. Numerical examples were performed for two-dimensional exterior acoustics to demonstrate the cost effectiveness of adaptive scheme.

2. Statement for exterior boundary-value problems of the Helmholtz equation

Let $D \subset D^d$ be an unbounded region, where d is the number of space dimensions, d can be 1, 2 or 3. The boundary of the domain D, denoted by B, is internal and assumed piecewise smooth as shown in Fig. 1(a). The outward unit vector normal to B is denoted by n. We assume that boundary, B, admits the partition [14,23]

$$B = B_g \cup B_h, \tag{1}$$

$$\phi = B_g \cap B_h. \tag{2}$$

We intend to study the effects of small disturbances to a given background flow in such a region, under the usual assumptions that led to the equations of acoustics. Harmonic analysis leads to a boundary-value problem for the Helmholtz equation (or reduced wave equation): Find u in the exterior domain, the spatial component for the acoustic pressure or velocity potential [14,23], such that

$$-\mathscr{L}u = f \quad \text{in } D, \tag{3}$$

$$u = g \quad \text{on } B_g, \tag{4}$$

$$\frac{\partial u}{\partial n} = \mathrm{i}kh \quad \text{on } B_h, \tag{5}$$

$$\lim_{r\to\infty} r^{\frac{1}{2}(d-1)}\left(\frac{\partial u}{\partial r} - \mathrm{i}ku\right) = 0 \quad \text{at } \infty, \tag{6}$$

where $\mathscr{L}u := \nabla^2 u + k^2 u$ is the Helmholtz operator, ∇^2 is the Laplace operator and $k \geqslant 0$ is the wave number; and in particular $\partial u/\partial n := \nabla u \cdot \mathbf{n}$ is the normal derivative and ∇ is the gradient operator; $\mathrm{i}^2 = -1$; r is the distance from the origin; and g and h are the prescribed boundary data. In the linearized equations of motion, velocity gradients produce a compression of the acoustic medium and pressure gradients are related to acceleration. Thus, if the dependent variable is, e.g., the acoustic pressure, then the Neumann boundary condition (5) represents a prescribed velocity distribution on that portion of the wet surface, where h is proportional to the velocity and the presence of $\mathrm{i}k$ is a consequence of differentiation with respect to time. Neumann boundary conditions are therefore very common in physical situations that entail *radiation*, and in the model problems and demonstrative examples that are subsequently considered we emphasize boundary conditions of this type. It should be noted that the analysis is valid for any combination of boundary conditions on the wet surface for the boundary-value problem (3)–(6), and by no means is it limited to Neumann problems. For *scattering* problems, a fixed rigid object is represented by a homogeneous Neumann boundary condition, often referred to as a hard scatter. Conversely, the homogeneous Dirichlet *boundary* condition, an appropriate representation of a site of pressure release, is termed a soft scatter. An impedance boundary condition is a linear combination of the two [14,23].

Eq. (6) stems from the *Sommerfeld radiation condition* which allows only solutions with outgoing waves at infinity to be admitted. This boundary condition implies an integral form, the Rellich–Sommerfeld radiation condition

$$\lim_{r\to\infty}\int_{B_r}\left|\frac{\partial u}{\partial r}-\mathrm{i}ku\right|^2\mathrm{d}B=0, \tag{7}$$

where B_r is the surface of a sphere with a radius r. The radiation condition requires energy flux at infinity to be positive, thereby guaranteeing that the solution to the boundary-value problem (3)–(6) is unique. Appropriate representation of this condition is crucial to the reliability of any numerical formulation of the problem. In this section, the statement of problem followed the paper by Stewart and Hughes [23] since they presented a typical formulation.

3. Burton and Miller formulation for exterior acoustics using the dual BEM

The governing equation for exterior acoustics is the Helmholtz equation as follows:

$$(\nabla^2+k^2)u(x_1,x_2)=0\quad (x_1,x_2)\in D, \tag{8}$$

where f in Eq. (3) is zero (no sources), and k is the wave number, which is angular frequency over the speed of sound. The boundary conditions can be either the Neumann or Dirichlet type. Based on the dual formulation, the dual equations for the boundary points are

$$\pi u(x)=\mathrm{CPV}\int_B T(s,x)u(s)\,\mathrm{d}B(s)-\mathrm{RPV}\int_B U(s,x)t(s)\,\mathrm{d}B(s),\quad x\in B, \tag{9}$$

$$\pi t(x)=\mathrm{HPV}\int_B M(s,x)u(s)\,\mathrm{d}B(s)-\mathrm{CPV}\int_B L(s,x)t(s)\,\mathrm{d}B(s),\quad x\in B, \tag{10}$$

where CPV, RPV and HPV denote the Cauchy principal value, the Riemann principal value and the Hadamard principal value, $t(s)=\partial u(s)/\partial n_s$, B denotes the boundary enclosing D and the explicit forms of the four kernels, U, T, L and M, can be found in [4,10,11]. The linear algebraic equations discretized from the dual boundary integral equations can be written as

$$[T_{pq}]\{u_q\}=[U_{pq}]\{t_q\}, \tag{11}$$

$$[M_{pq}]\{u_q\}=[L_{pq}]\{t_q\}, \tag{12}$$

where $\{u_q\}$ and $\{t_q\}$ are the boundary potential and flux, and the subscripts p and q correspond to the labels of the collocation element and integration element, respectively. The influence coefficients of the four square matrices $[U]$, $[T]$, $[L]$ and $[M]$ can be represented as [5,6]

$$U_{pq}=\mathrm{RPV}\int_{Bq}U(s_q,x_p)\,\mathrm{d}B(s_q), \tag{13}$$

$$T_{pq}=-\pi\delta_{pq}+\mathrm{CPV}\int_{B_q}T(s_q,x_p)\,\mathrm{d}B(s_q), \tag{14}$$

$$L_{pq}=\pi\delta_{pq}+\mathrm{CPV}\int_{B_q}L(s_q,x_p)\,\mathrm{d}B(s_q), \tag{15}$$

$$M_{pq}=\mathrm{HPV}\int_{B_q}M(s_q,x_p)\,\mathrm{d}B(s_q), \tag{16}$$

where B_q denotes the qth element and $\delta_{pq} = 1$ if $p = q$; otherwise it is zero. In order to avoid the problem of fictitious frequency, the Burton and Miller formulation [2] is employed by combining the dual equations as follows:

$$\left\{[T_{pq}] + \frac{\mathrm{i}}{k}[M_{pq}]\right\}\{u_q\} = \left\{[U_{pq}] + \frac{\mathrm{i}}{k}[L_{pq}]\right\}\{t_q\}. \tag{17}$$

For all wave numbers, Eq. (17) can work well [1].

4. Pointwise error indicators using the dual BEM

Based on the Burton and Miller formulation, the exterior acoustics can be solved for all wave numbers. By substituting the solved boundary unknowns in Eq. (17) into Eqs. (9) and (10), we have the two residuals for the error indicators,

$$\varepsilon_{UT} = \mathrm{CPV}\int_B T(s,x)u(s)\,\mathrm{d}B(s) - \mathrm{RPV}\int_B U(s,x)t(s)\,\mathrm{d}B(s) - \pi u(x), \quad x \in B, \tag{18}$$

$$\varepsilon_{LM} = \mathrm{HPV}\int_B M(s,x)u(s)\,\mathrm{d}B(s) - \mathrm{CPV}\int_B L(s,x)t(s)\,\mathrm{d}B(s) - \pi t(x), \quad x \in B. \tag{19}$$

Theoretically, ε_{UT} and ε_{LM} in Eqs. (18) and (19) are both zeros if no numerical error is involved. In real calculations, the two residuals are not zeros when collocating points along the boundary as shown below

$$\{\varepsilon_{UT}\} = [T_{pq}]\{u_q\} - [U_{pq}]\{t_q\}, \tag{20}$$

$$\{\varepsilon_{LM}\} = [M_{pq}]\{u_q\} - [L_{pq}]\{t_q\}, \tag{21}$$

The two values are the important information for the error indicators. If the exact solution, u_e, is available, the third error indicator along the boundary can be defined for comparisons as

$$\varepsilon_{\mathrm{ex}} = |u - u_\mathrm{e}|, \tag{22}$$

and

$$\varepsilon_{\mathrm{ex}} = |t - t_\mathrm{e}|, \tag{23}$$

for the Neumann and Dirichlet problems, respectively.

5. Adaptive scheme in dual BEM

The role of the adaptive tactical procedure is to determine the region where the elements should be refined. This *algorithm* is very strongly dependent on error estimation and the mesh refinement scheme. The reference value, error *convergence* and equilibrium criterion methods [17] have been popular adaptive tactics for the h-refinement scheme [3,16,17,20]. In the case of the reference value method, elements are refined when their errors are larger than the prescribed reference value. Denoting the error at the ith element by ε_i, the reference value $\bar{\varepsilon}$ can be defined as

$$\bar{\varepsilon} = \text{average of } \varepsilon_i, \tag{24}$$

or

$$\bar{\varepsilon} = \eta \max(\varepsilon_i) \quad (0 < \eta < 1). \tag{25}$$

In this paper, the former value in Eq. (24) is chosen because it is difficult to specify the value of η in Eq. (25) adequately.

Since the error estimator and adaptive tactics can be obtained, the self adaptive mesh refinement process can be implemented. The flowchart of the self adaptive mesh refinement is shown in Fig. 2. Fig. 2 provides a simple illustration of how adaptive BEM works; all adaptive computations fit more or less into this general framework. The algorithm is similar to [23] by using BEM instead of FEM. The flowchart shows how the various components of adaptivity works together to put the efficient elements in the meshes. Then a posteriori error estimator takes the Burton and Miller boundary solution as input arid computes an estimate of the solution error by using the dual equations. According to the estimated error distribution, a new and more efficient mesh can be constructed. The mesh generator then creates the adaptive mesh with the requested size distribution, and the process repeats until a stopping criterion is satisfied. The coarse mesh is initiated in the beginning, and drives the adaptive refinement through the selection of smaller and smaller error tolerance (prescribed reference value) in the iteration. Usually, three or four iterations are sufficient. Efficiency is attained by placing more elements in areas where errors are large. In doing so, the adaptive strategy attempts to compute a distribution of element size such that the error is redistributed among the elements in the mesh. Based on the reference value method for the self adaptive technique, the minimum number of elements can be obtained under the requirement of error tolerance. Thus, the measure of error

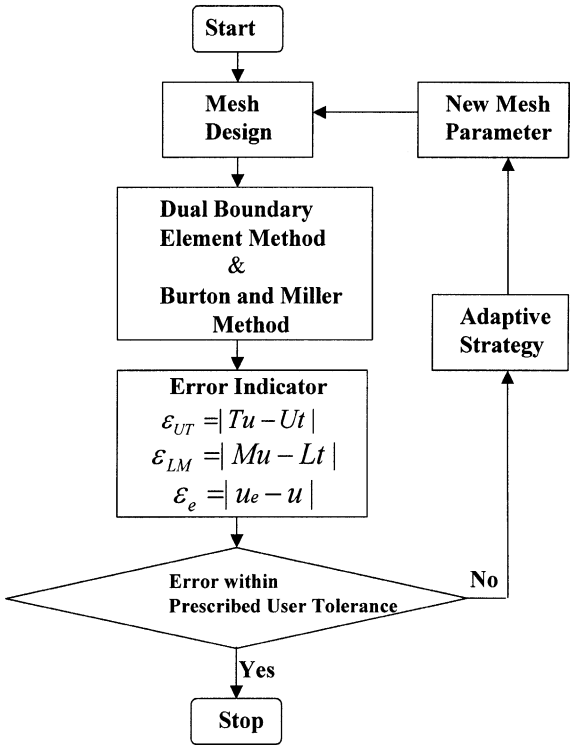

Fig. 2. Flowchart of adaptive mesh generation.

must be specified. Although many measures of error have been used, e.g., (a) pointwise error, (b) max norm: $\|u-u_e\| = \max_{a\leqslant x\leqslant b}|u(x)-u_e(x)|$ and (c) L_2 norm: $\|u-u_e\| = \{\sqrt{\int_a^b |u-u_e|^2\,dx}\}$, the L_2 norm along the boundary has been adopted in this paper.

6. Numerical examples

Case 1: nonuniform radiation problem by an infinite cylinder (Neumann boundary condition).

The problem was chosen because the exact solution is known [13]. It is therefore a good model problem to test the effectiveness of the error estimator and adaptive strategy since the solution is directional and effect of adaptivity may be significant. The example with the Neumann boundary condition is shown in Fig. 3. The analytical solution is

$$u(r,\theta) = \frac{2}{\pi}\sum_{n=0}^{\infty}{}' \frac{-1}{k}\frac{\sin(n\alpha)}{n}\frac{H_n^{(1)}(kr)}{H_n^{(1)\prime}(ka)}\cos(n\theta), \tag{26}$$

where $'$ is the Neumann factor, $H_n^{(1)}(kr)$ and $H_n^{(1)\prime}(ka)$ are the Hankel functions with the nth order and its derivative, respectively. The contour plots for the real-part solutions are shown in Fig. 4 for the case of $\alpha = \pi/9$. It indicates that numerical results agree well with the analytical solution. Also, it is interesting to find that the irregular frequencies in Fig. 5 occur as predicted theoretically by Chen and Kuo [8]. This confirms the conclusion in [7,8] that the irregular frequencies depend on the integral formulation (*UT* or *LM* method) instead of the types of boundary conditions (Dirichlet or Neumann). For the case of $ka = 1$, we can construct the three error tracking curves in Fig. 6(a) for the initial mesh. The consistent behavior among the three error indicators can be found. Burton and Miller method can work well for all wave numbers and the *UT* and *LM* results agree well except at the irregular wave numbers as shown in Fig. 5. It is found that irregular values occur at J_n^m, the mth zeros of the nth order Bessel function, $J_n(ka)$, for the *UT* formulation, while the *LM* formulation has the irregular values of $J_n'^m$, the mth zeros of $J_n'(ka) = 0$. According to the adaptive scheme, meshes of 12, 20 and 28 elements are successively created in Fig. 7. The higher density of mesh near the boundary with discontinuous potential is found in a consistent way of engineering judgement. The error tracking curve for the three adaptive meshes is shown in Fig. 6(b)–(d),

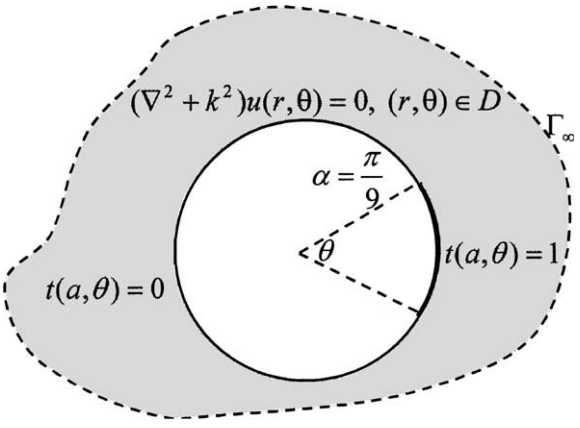

Fig. 3. The non-uniform radiation problem (Neumann condition) for a cylinder.

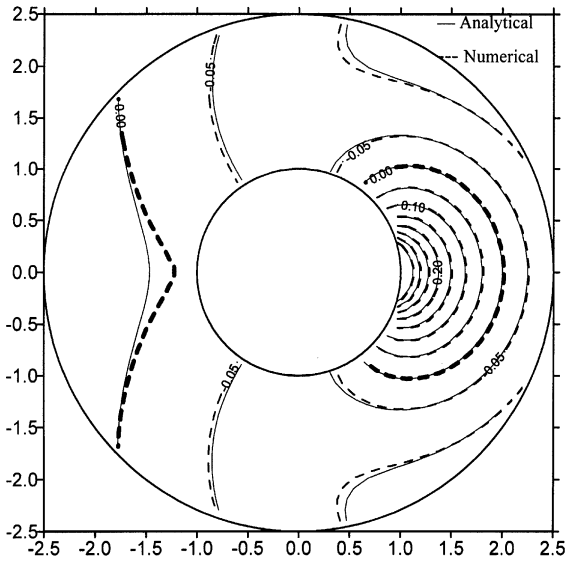

Fig. 4. The contour plot for the real-part solutions (analytical solution: dashed line, numerical result: solid line, $ka = 1$).

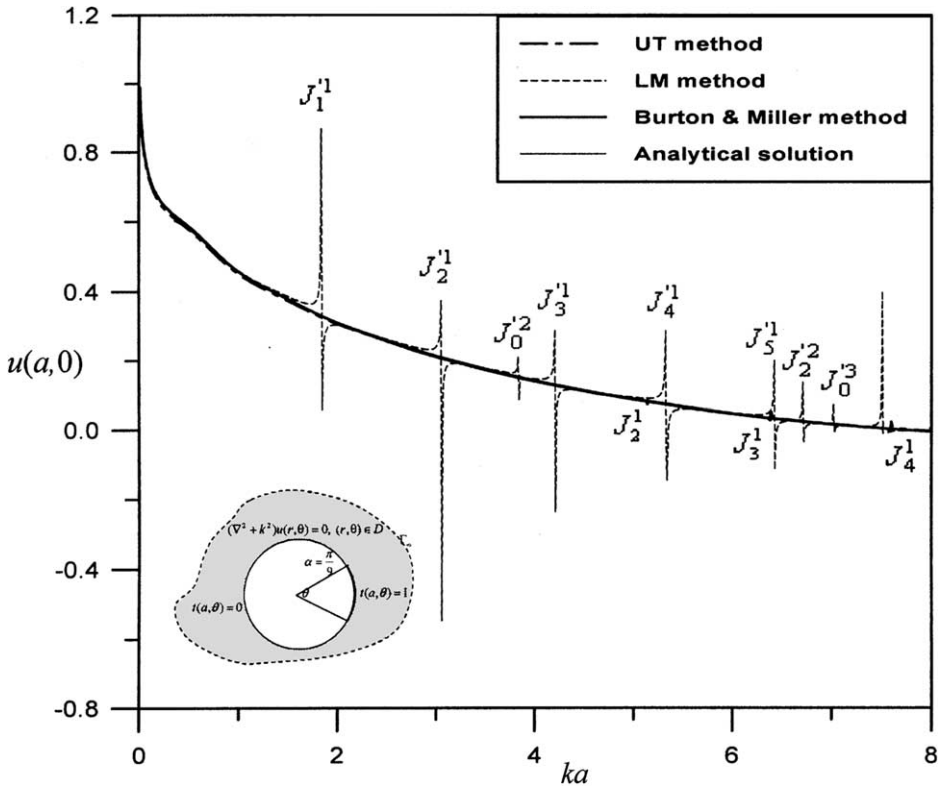

Fig. 5. The positions of irregular values using different methods.

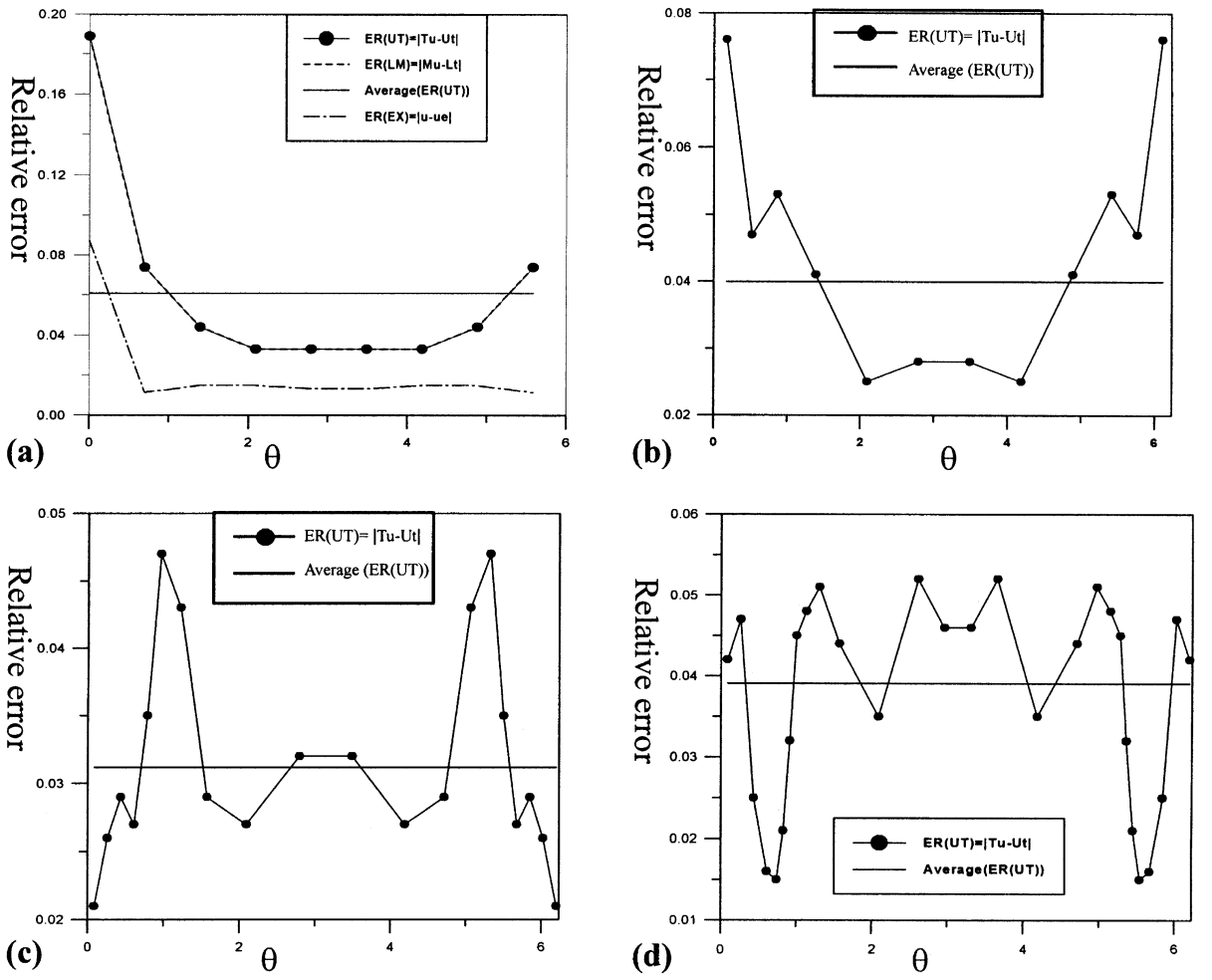

Fig. 6. Error tracking curves (a) 9 elements, (b) 12 elements, (c) 20 elements, (d) 28 elements.

respectively. The average error $[ER(UT)]$ for Fig. 6(d) using 28 elements is found to be larger than that of Fig. 6(c) using 20 elements. Since the error term is obtained from the inconsistency in substituting boundary data into the UT equation instead of comparison with the exact solution, it is useful that the values of the error on each elements represent as a relative quantity in comparison with the other elements in the same level of mesh. For demonstration, only Fig. 6(a) shows the four error indicators. The values of error norm using the adaptive mesh (Fig. 7) are less than those of the uniform meshes (Fig. 8) as shown in Fig. 9.

Case 2: scattering problem by an infinite cylinder (Neumann boundary condition).

By changing the radiation problem in case 1 into the scattering problem as shown in Fig. 10 [12,23], we have the analytical solution

$$u(r,\theta) = -\frac{J_0'(ka)}{H_0^{(1)'}(ka)} H_0^{(1)}(kr) - 2\sum_{n=1}^{\infty} i^n \frac{J_n'(ka)}{H_n^{(1)'}(ka)} H_n^{(1)}(kr)\cos(n\theta). \tag{27}$$

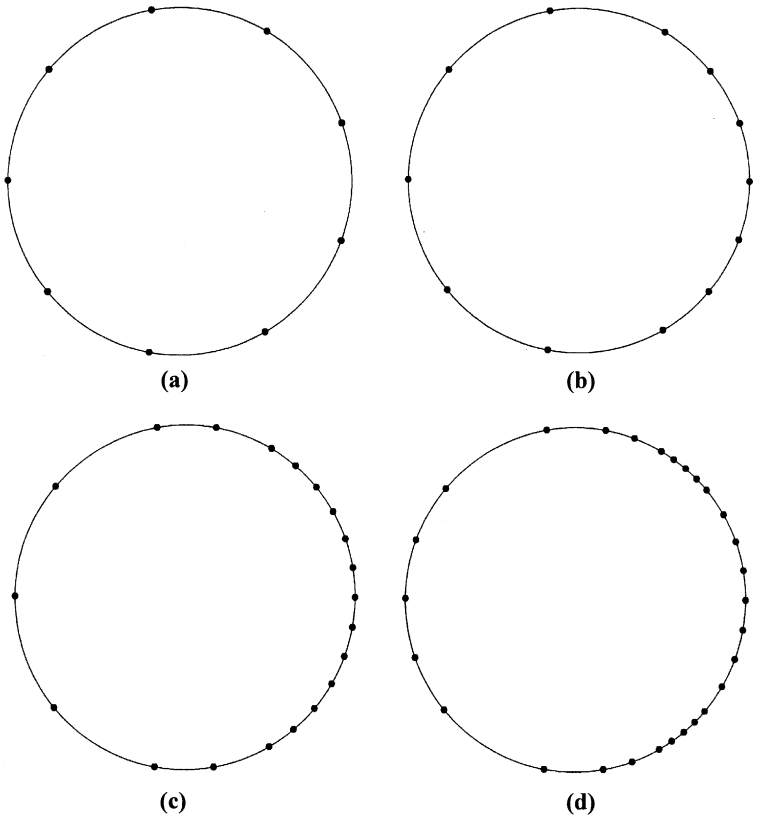

Fig. 7. Adaptive meshes: (a) 9 elements, (b) 12 elements, (c) 20 elements, (d) 28 elements.

Fig. 11 shows the contour plots for the real-part solutions for the case of $ka = 4\pi$. The positions where the irregular values occur can be found in Fig. 12 for the solution $u(a, 0)$ versus k by using either the UT or the LM equation only. Solution using the adaptive mesh refinement converge to the exact solution as shown in Fig. 13. The results of the dual BEM in comparison with the analytical solution and the DtN results [23] make a good agreement. Both the real and imaginary components for u on $r = 2a$ are plotted for comparison with the DtN results by FEM, along with the corresponding analytical values (due to symmetry, only $0 \leqslant \theta \leqslant \pi$ is shown). These results demonstrate the convergence of the solution using adaptive BEM mesh refinement. The comparison of error norms between the uniform mesh and the adaptive mesh is shown in Fig. 14. It is found that the adaptive mesh solution approaches the exact solution more efficiently than uniform mesh solution does by using the same number of elements.

Case 3: scattering problem by a square rod (Neumann boundary condition).

Having demonstrated the adaptive technology on the infinite circular cylinder, we proceed to a problem in which exact solution is not available [23]. Due to nonsmooth boundary of four corners in the square, the scattering by the infinite square rod of area 4 m^2 is more directional and thus leads itself more to adaptivity. Solution contours of $\mathrm{Re}(u)$ for $ka = 4\pi$ are shown in Fig. 15. In Fig. 16, the imaginary component of u on the radius $r = 1/0.425$ is plotted for comparison with the DtN FEM results. Solutions of the initial mesh and the successive adaptive meshes are also compared with.

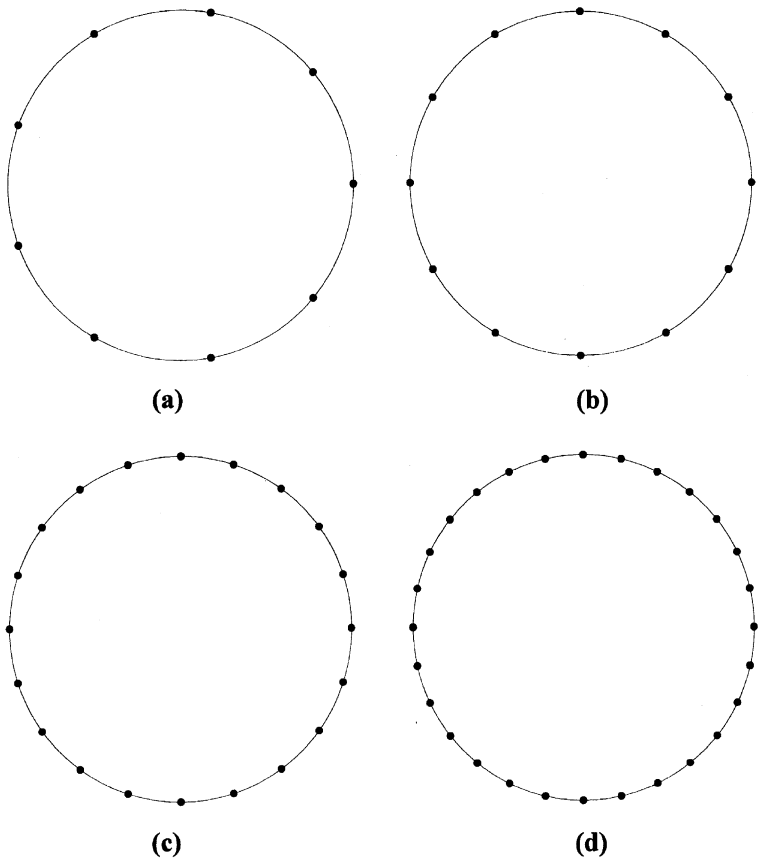

Fig. 8. Uniform meshes: (a) 9 elements, (b) 12 elements, (c) 20 elements, (d) 28 elements.

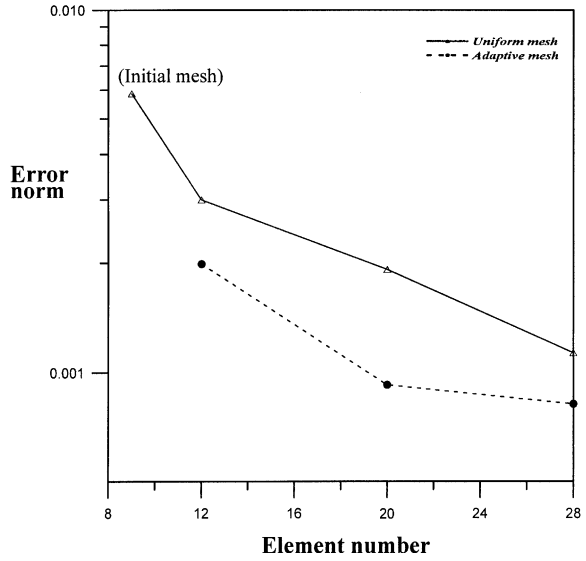

Fig. 9. Comparison of error norms using uniform mesh and adaptive mesh.

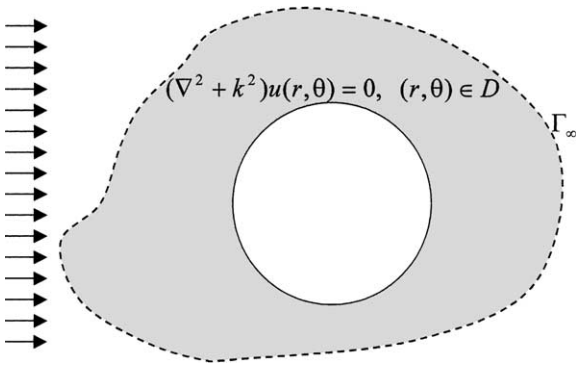

Fig. 10. The scattering problem (Neumann condition) for a cylinder.

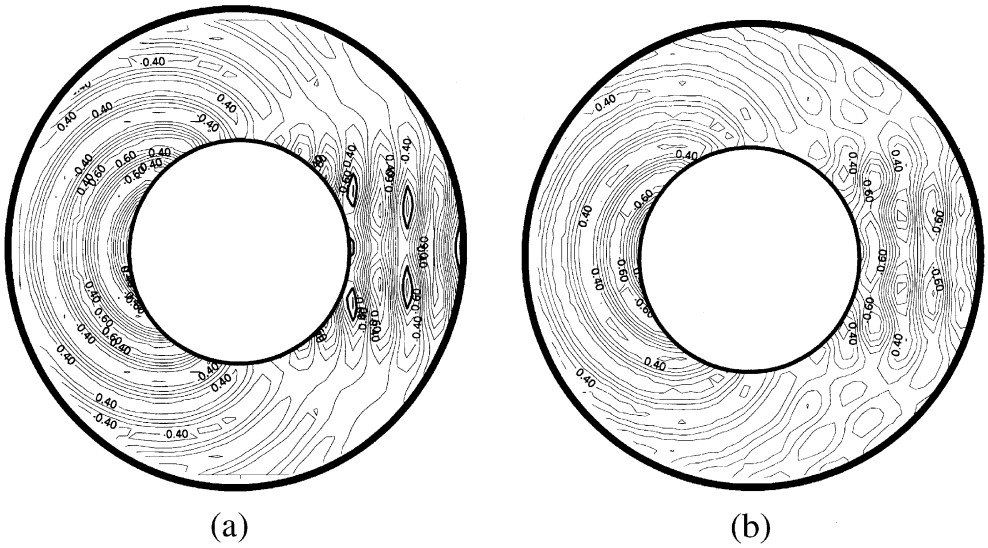

Fig. 11. The contour plot for the real-part solutions (a) analytical solution, (b) numerical results.

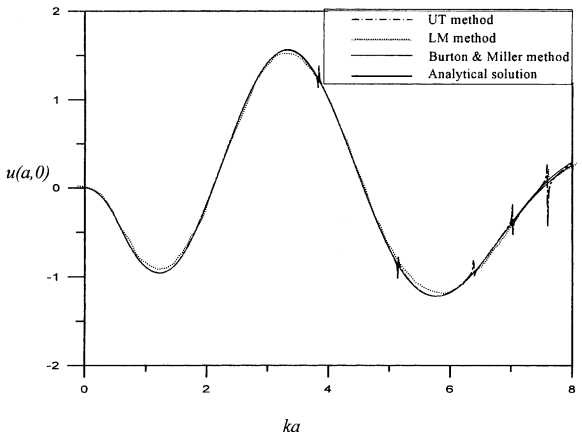

Fig. 12. The positions of irregular values using different methods.

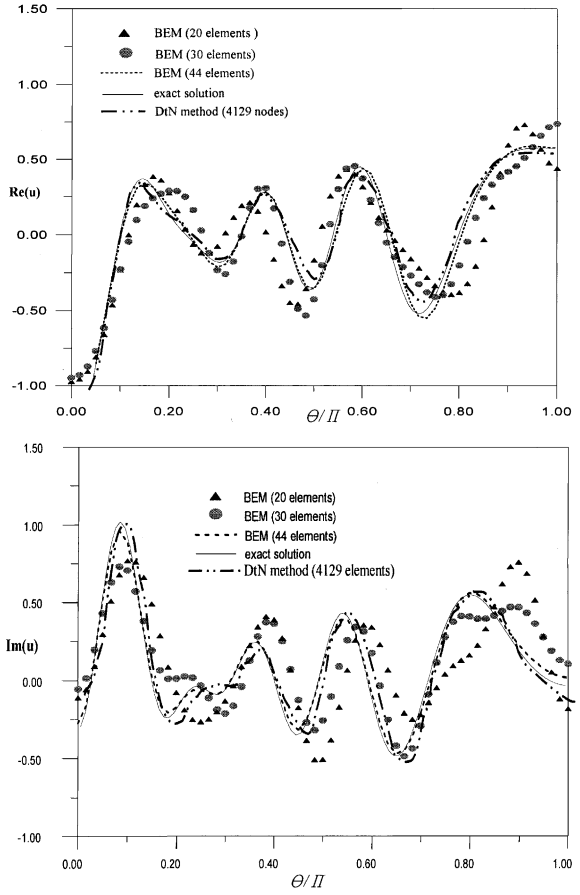

Fig. 13. Plane wave scattering by an infinite circular cylinder, $ka = 4\pi$, convergence with mesh refinement of $\mathrm{Re}(u)$ and $\mathrm{Im}(u)$ at $r = 2a$ (only the top half of the boundary is plotted).

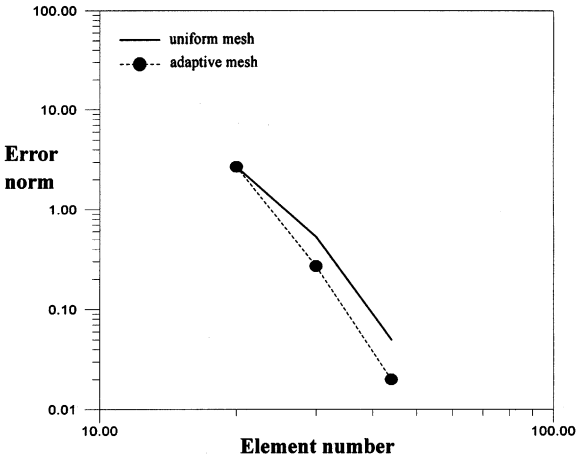

Fig. 14. Comparison of error norms using uniform mesh and adaptive mesh.

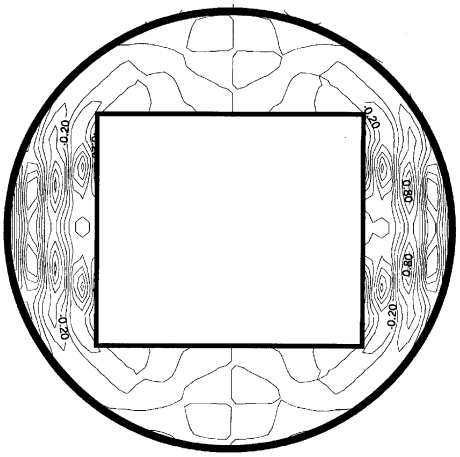

Fig. 15. Plane wave scattering by an infinite square rod, the contour plot for the real part solution, $ka = 4\pi$.

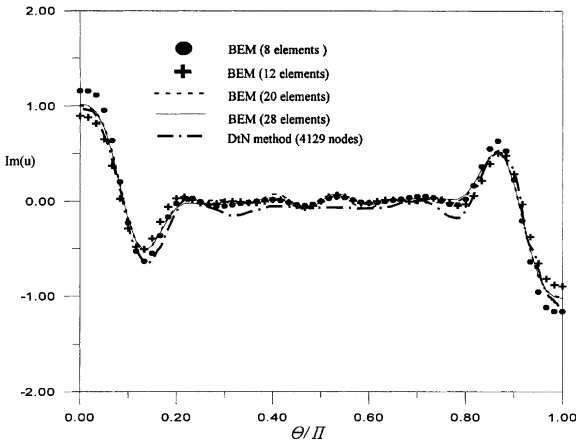

Fig. 16. Plane wave scattering by an infinite square rod, $ka = 4\pi$, imaginary part of solution at $r = 2a$ (only the top half of the boundary is plotted).

7. Conclusions

In this paper, we demonstrated boundary element solution—adaptive acoustics methodologies on model time-harmonic exterior acoustics problems in two dimensions. The results indicate that adaptivity can provide an increase in mesh efficiency for the Helmholtz problems at moderate wave numbers. The adaptive computations involved the Burton and Miller formulation and the dual BEM. The error tracking curves were *successfully* constructed. According to the error tracking curves, adaptive strategy can be implemented. Based on the posteriori pointwise error distribution, adaptive mesh was generated to approach the exact solution more efficiently than uniform mesh does.

Acknowledgements

The *financial* support from NSC projects with Grants no. NSC 89-2211-E-019-003 and NSC 90-2211-E-019-021 is highly appreciated.

References

[1] S. Amini, On the choice of the coupling parameter in boundary integral formulation for the exterior acoustic problem, Appl. Anal. 35 (1990) 75–92.
[2] A.J. Burton, G.F. Miller, The application of integral equation methods to numerical solution of some exterior boundary value problems, Proc. Roy. Soc. London Ser. A 323 (1971) 201–210.
[3] C. Carstensen, D. Estep, E.P. Stephan, h-adaptive boundary element schemes, Comput. Mech. 15 (1995) 372–383.
[4] J.T. Chen, H.K. Hong, Boundary Element Method, second ed., New World Press, Taipei, Taiwan, 1992 (in Chinese).
[5] J.T. Chen, H.K. Hong, S.W. Chyuan, Boundary element analysis and design in seepage flow problems with sheetpiles, Finite Elem. Anal. Des. 17 (1994) 1–20.
[6] J.T. Chen, M.T. Liang, S.S. Yang, Dual boundary integral equation for exterior problems, Engrg. Anal. Bound. Elem. 16 (1995) 333–340.
[7] J.T. Chen, On fictitious frequencies using dual series representation, Mech. Res. Commun. 25 (1998) 529–534.
[8] J.T. Chen, S.R. Kuo, On fictitious frequencies using circulants for radiation problems of a cylinder, Mech. Res. Commun. 27 (2000) 49–58.
[9] J.T. Chen, C.T. Chen, K.H. Chen, I.L. Chen, On fictitious frequencies using dual BEM for nouniform radiation problems of a cylinder, Mech. Res. Commun. 27 (6) (2000) 685–690.
[10] J.T. Chen, H.-K. Hong, Review of dual boundary element methods with emphasis on hypersingular integrals and divergent series, ASME, Appl. Mech. Rev. 52 (1999) 17–33.
[11] J.T. Chen, K.H. Chen, Dual integral formulation for determining the acoustic modes of a two-dimensional cavity with a degenerate boundary, Engrg. Anal. Bound. Elem. 21 (1998) 105–116.
[12] I. Harari, P.E. Barbone, J.M. Montgomery, Finite element formulations for exterior problems: application to hybrid methods, non-reflecting boundary conditions and infinite elements, Int. J. Numer. Meth. Engrg. 40 (1997) 2791–2805.
[13] I. Harari, P.E. Barbone, M. Slavutin, R. Shalom, Boundary infinite elements for the Helmholtz equation in exterior domains, Int. J. Numer. Meth. Engrg. 41 (1998) 1105–1131.
[14] I. Harari, T.J.R. Hughes, A cost comparison of boundary element and finite element methods for problems of time-harmonic structural acoustics, Comput. Meth. Appl. Mech. Engrg. 97 (1992) 77–102.
[15] M.S. Ingber, A.K. Mitra, Grid optimization for the boundary element method, Int. J. Numer. Meth. Engrg. 23 (1986) 2121–2136.
[16] N. Kamiya, Y. Aikawa, K. Kawaguchi, Adaptive boundary element for the problem with mixed boundary condition, in: C.A. Brebbia, S. Kim, T.A. Osswald, H. Power (Eds.), Boundary Elements XVII, 1995.
[17] E. Kita, N. Kamiya, Recent studies on adaptive boundary element methods, Adv. Engrg. Software 19 (1994) 21–32.
[18] D.W. Kelly, R.J. Mills, J.A. Reizes, A.D. Mills, A posteriori estimates of the solution caused by discretization in the finite element, finite difference and boundary element methods, Int. J. Numer. Meth. Engrg. 24 (1987) 1921–1939.
[19] M.T. Liang, J.T. Chen, S.S. Yang, Error estimation for boundary element method, Engrg. Anal. Bound. Elem. 23 (1999) 257–265.
[20] R.P. Leal, C.A. Mota Soares, Adaptive boundary element method for bidimensional elasticity, Comp. Struct. 30 (1988) 841–844.
[21] G. Menon, G.H. Paulino, S. Mukherjee, Analysis of hypersingular residual error estimation in the boundary element method for potential, Comput. Meth. Appl. Mech. Engrg. 173 (1999) 449–473.
[22] G.H. Paulino, L.J. Gray, V. Zarikian, Hypersingular residual—A new method for error estimation in the boundary element method, Int. J. Numer. Meth. Engrg. 39 (1996) 2005–2029.
[23] J.R. Stewart, T.J.R. Hughes, h-adaptive finite element computation of time-harmonic exterior accoustics problems in two dimension, Comp. Meth. Appl. Mech. Engrg. 146 (1997) 65–89.
[24] V. Zarikian, L.J. Gray, G.H. Paulino, Pointwise error estimates for boundary element calculations, in: C.A. Brebbia, A.J. Kassab (Eds.), Boundary Element Technology IV, Computational Mechanics Publications, 1994, pp. 253–260.